

Chapter 1

Basic Principles of the Electrochemical Mineralization of Organic Pollutants for Wastewater Treatment

Agnieszka Kapałka, György Fóti, and Christos Comninellis

1.1 Introduction

Biological treatment of polluted water is the most economical process and it is used for the elimination of “readily degradable” organic pollutants present in wastewater. The situation is completely different when the wastewater contains toxic and refractory (resistant to biological treatment) organic pollutants. One interesting possibility is to use a coupled process: partial oxidation – biological treatment. The goal is to decrease the toxicity and to increase the biodegradability of the wastewater before the biological treatment. However, the optimization of this coupled process is complex and usually complete mineralization of the organic pollutants is preferred. The mineralization of these organic pollutants can be achieved by complete oxidation using oxygen at high temperature or strong oxidants combined with UV radiation. Depending on the operating temperature, the type of used oxidant, and the concentration of the pollutants in the wastewater, the mineralization can be classified into three main categories:

- (a) *Incineration*. Incineration takes place in the gas phase at high temperature (820–1,100°C). Its main characteristic is a direct combustion with excess oxygen from air in a flame. The process is nearly instantaneous. Incineration by-products are mainly in the gas (including NO_x, SO₂, HCl, dioxins, furans, etc.) and solid phases (bottom and fly ashes). The technology is applied mainly for concentrated wastewater with chemical oxygen demand, COD > 100 g/L.
- (b) *Wet air oxidation process (WAO)*. WAO can be defined as the oxidation of organic pollutants in an aqueous media by means of oxygen from air at elevated temperature (250–300°C) and high pressure (100–150 bar). Usually Cu²⁺ is used as a catalyst in order to increase the reaction rate. The efficiency of the mineralization can be higher than 99% and the main by-products formed in the aqueous phase after the treatment are acetone, methanol, ethanol, pyridine, and

A. Kapałka (✉)

Institute of Chemical Sciences and Engineering, Ecole Polytechnique
Fédérale de Lausanne (EPFL), CH-1015 Lausanne, Switzerland
e-mail: agnieszka.cieciwa@epfl.ch

methanesulfonic acid. The technology is attractive for treatment of wastewater with moderate concentration. The optimal COD is in the domain: $50 \text{ g/L} > \text{COD} > 15 \text{ g/L}$.

- (c) *Oxidation with strong oxidants*. The oxidation of organic pollutants with strong oxidants (H_2O_2 , O_3) takes place generally at room temperature. In order to increase the efficiency of mineralization, the oxidation takes place in the presence of catalyst and UV radiation. This technology is interesting for the treatment of dilute wastewater with $\text{COD} < 5 \text{ g/L}$.

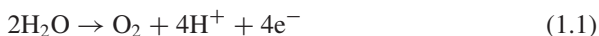
The electrochemical method for the mineralization of organic pollutants is a new technology and has attracted a great deal of attention recently. This technology is interesting for the treatment of dilute wastewater ($\text{COD} < 5 \text{ g/L}$) and it is in competition with the process of chemical oxidation using strong oxidants. The main advantage of this technology is that chemicals are not used. In fact, only electrical energy is consumed for the mineralization of organic pollutants. Besides our contribution in this field (Comninellis and Plattner 1988; Comninellis and Pulgarin 1991; Seignez et al. 1992; Comninellis 1992; Comninellis and Pulgarin 1993; Pulgarin et al. 1994; Comninellis 1994; Comninellis and Nerini 1995; Simond et al. 1997; Fóti et al. 1997; Ouattara et al. 2004), many other research groups are very active in this promising technology (Comninellis and De Battisti 1996; Iniesta et al. 2001a; Chen et al. 2003; Ouattara et al. 2003; Zanta et al. 2003; Polcaro et al. 2004; Brillas et al. 2004; Haenni et al. 2004; Martinez-Huitle et al. 2004; Polcaro et al. 2005; Chen et al. 2005; Boye et al. 2006).

The aim of the present work is to elucidate the basic principles of the electrochemical mineralization (EM) using some model organic pollutants. The following points will be treated:

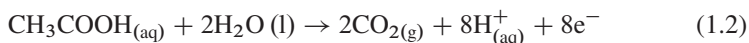
- Thermodynamics of the electrochemical mineralization (EM) of organics
- Mechanism of the electrochemical oxygen transfer reaction (EOTR)
- Influence of anode material on the reactivity of electrolytic hydroxyl radicals
- Determination of the current efficiency in the electrochemical oxidation process
- Kinetic model of organics mineralization on BDD anodes
- Intermediates formed during the EM process using BDD
- Electrical energy consumption in the EM process
- Optimization of the EM process using BDD
- Fouling and corrosion of BDD anodes.

1.2 Thermodynamics of the Electrochemical Mineralization

Thermodynamically, the electrochemical mineralization (EM) of any soluble organic compound in water should be achieved at low potentials, widely before the thermodynamic potential of water oxidation to molecular oxygen (1.23 V/SHE under standard conditions) as it is given by (1.1):



A typical example of EM is the anodic oxidation of acetic acid to CO_2 (1.2):



The thermodynamic potential of this reaction E^0 (V) can be calculated using (1.3):

$$E^0 = \frac{-\Delta_r G^0}{nF}, \quad (1.3)$$

where $\Delta_r G^0$ (J mol^{-1}) is the standard free energy of the reaction, n is the number of exchanged electrons ($n = 8$), and F is Faraday's constant (C mol^{-1}). The standard free energy of the reaction $\Delta_r G^0$ can be calculated from the tabulated values of the standard free energy of formation ($\Delta_f G^0$) of both reactants and products (1.4):

$$\begin{aligned} -\Delta_r G^0 &= 2\Delta_f G^0(\text{CO}_2) - \Delta_f G^0(\text{CH}_3\text{COOH}) - 2\Delta_f G^0(\text{H}_2\text{O}), \quad (1.4) \\ -\Delta_r G^0 &= 2 \times (-394.4 \times 10^3) - (-399.6 \times 10^3) - 2 \times (-237.13 \times 10^3) \\ &= 85.1 \times 10^3 \text{ J mol}^{-1}. \end{aligned}$$

From the calculated standard free energy, the thermodynamic potential of reaction (1.2) under standard conditions (1 mol dm^{-3} , CH_3COOH , $P = 1 \text{ atm}$, $T = 25^\circ\text{C}$) can be calculated using (1.3):

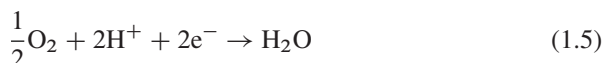
$$E^0 = \frac{-\Delta_r G^0}{nF} = \frac{85.1 \times 10^3}{8 \cdot 96485} = 0.11 \text{ V/SHE}.$$

Similarly, the thermodynamic potential for EM of some model organic compounds (alcohols, carboxylic acids, ketenes, phenols, and aromatic acids) can be calculated. Typical values are reported in Table 1.1. This table shows that the thermodynamic potential for EM of organics never exceeds 0.2 V/SHE.

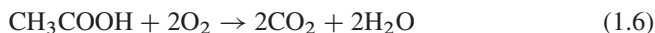
Table 1.1 Standard free energy $\Delta_f G^0$, thermodynamic potential for organics mineralization E^0 and thermodynamic cell potential ΔE_{cell}^0 calculated for various organic compounds

Organic compound	$\Delta_f G^0$ (kJ mol^{-1})	E^0 (V/SHE)	ΔE_{cell}^0 (V/SHE)
CH_3OH	-17.2	0.030	1.20
$\text{C}_2\text{H}_5\text{OH}$	-99.6	0.086	1.14
$\text{C}_3\text{H}_7\text{OH}$	-173.2	0.100	1.13
CH_3COOH	-85.1	0.110	1.12
CH_3COCH_3	-157.9	0.102	1.13
$\text{C}_6\text{H}_5\text{OH}$	-292.9	0.108	1.13
$\text{C}_6\text{H}_5\text{COOH}$	-330.1	0.114	1.11

Taking into consideration this result, it will be theoretically possible to treat an aqueous organic pollutants stream as a fuel cell with co-generation of electrical energy. In this device, the organic pollutant is oxidized at the anode [(1.2) in case of acetic acid] and oxygen is reduced at the cathode (1.5):



The total reaction of this fuel cell, considering acetic acid as a fuel, is given by (1.6):



The standard free energy change of this fuel cell can be calculated from the tabulated standard free energy of formation of reactant and products:

$$\begin{aligned} \Delta_r G^0 &= 2\Delta_f G^0(\text{CO}_2) + 2\Delta_f G^0(\text{H}_2\text{O}) - \Delta_f G^0(\text{CH}_3\text{COOH}), \\ \Delta_r G^0 &= 2 \times (-394.4 \times 10^3) + 2 \times (-237.13 \times 10^3) - (-399.6 \times 10^3) \\ &= -863.5 \times 10^3 \text{ J mol}^{-1}. \end{aligned}$$

Finally, the standard thermodynamic potential of the cell, based on (1.6) (i.e., incineration of the pollutant with co-generation of energy), can be calculated using the relation:

$$E_{\text{cell}}^0 = \frac{-\Delta_r G^0}{nF} = \frac{-(-863.5 \times 10^3)}{8 \cdot 96485} = 1.12 \text{ V}.$$

In Table 1.1, the thermodynamic cell potentials calculated for some other organics are given. Values close to 1 V can be achieved under standard conditions. Figure 1.1 shows a schematic presentation of a hypothetical fuel cell for the incineration of organic pollutants with co-generation of electrical energy.

In contrast to these promising thermodynamic data, the kinetics of the electrochemical mineralization is very slow and in practice it can be achieved close to the thermodynamic potentials only in very limited cases. In fact, only platinum-based electrodes can allow EM of simple C₁ organic compounds. A typical example is the use of Pt–Ru catalyst in the electrochemical mineralization of methanol.

In conclusion, in the actual state of the art, the electrochemical mineralization of organic pollutants with co-generation of electrical energy is not feasible due to the lack of active electrocatalytic anode material. However, recently we have demonstrated that the electrochemical mineralization of organics can be achieved on some electrode material by electrolysis at potentials largely above the thermodynamic potential of oxygen evolution (1.23 V/SHE under standard conditions). Even if in this process electrical energy is consumed, this system opens new possibilities for the treatment at room temperature of very toxic organic pollutants present in

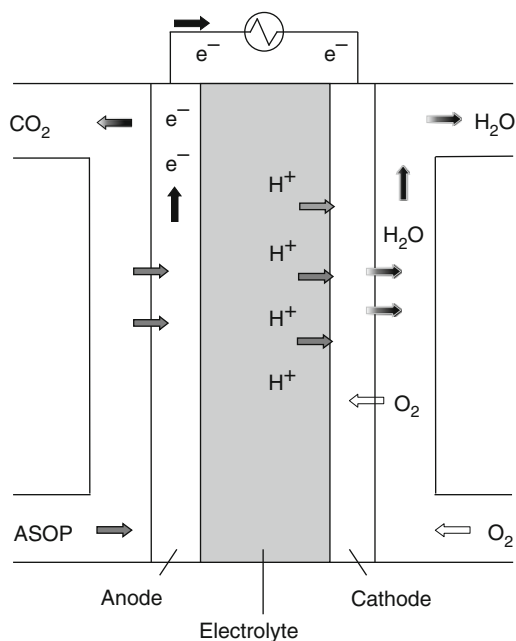


Fig. 1.1 Schematic representation of a hypothetical fuel cell for the mineralization of organic pollutants; *ASOP* aqueous solution of organic pollutants

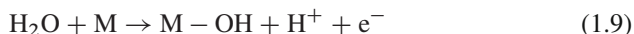
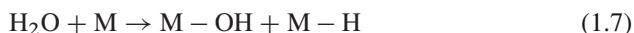
industrial wastewater (Boye et al. 2004; Gandini et al. 2000; Rodrigo et al. 2001; Panizza et al. 2001a, b; Iniesta et al. 2001b; Fryda et al. 1999; Montilla et al. 2001; Bellagamba et al. 2002; Boye et al. 2002; Montilla et al. 2002).

1.3 Mechanism of the Electrochemical Mineralization

In general, anodic oxidation reactions are accompanied by transfer of oxygen from water to the reaction products. This is the so-called EOTR. A typical example of EOTR is the EM of acetic acid (1.2). In this anodic reaction, water is the source of oxygen atoms for the complete oxidation of acetic acid to CO_2 . However, in order to achieve the EOTR, water should be activated. Depending on electrode material, there are two main possibilities for the electrochemical activation of water in acid media (1) by dissociative adsorption of water in the potential region of the thermodynamic stability of water (fuel cell regime) and (2) by electrolytic discharge of water at potentials above its thermodynamic stability (electrolysis regime).

1.3.1 Activation of Water by Dissociative Adsorption

According to this mechanism, in acid media, water is dissociatively adsorbed on the electrode (1.7) followed by hydrogen discharge (1.8) resulting in the formation of chemisorbed (chemically bonded) hydroxyl radicals on the anode surface (1.9):



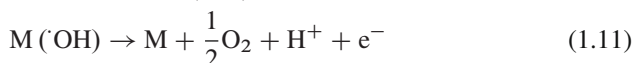
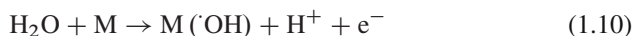
The reaction can take place at anode potentials largely lower than the thermodynamic potential of water oxidation to oxygen (1.23 V/SHE under standard conditions). However, in order to achieve the dissociative activation of water (1.7), electrocatalytic electrodes are needed. In fact, the dissociative adsorption of water can be achieved only at electrodes (M) on which the bonding energy of M–OH and M–H exceeds the dissociation energy of water to $\text{H}^\bullet + \text{HO}^\bullet$. This is the case of Pt–Ru-based electrodes on which water activation can be achieved at 0.2–0.3 V/SHE.

The EOTR between the organic compound (R) and the hydroxyl radicals take place at the electrode surface (both adsorbed) according to a Langmuir–Hinshelwood type mechanism. This process has been extensively studied mainly for fuel cell applications. However, as it has been reported in Sect. 1.2, it is limited for simple C_1 organic compounds (methanol, formic acid). Furthermore, there are problems with electrode deactivation due to CO chemisorption on the electrode active sites.

We stress again here that in the actual state of the art, the EM of organic pollutants with simultaneous production of electrical energy (fuel cell regime) is not feasible due to the lack of active electrocatalytic anode material. Bio-electrocatalysis is a new active field and can overcome this problem as it has been demonstrated recently in the development of bio-fuel cells.

1.3.2 Activation of Water by Electrolytic Discharge

According to this mechanism, in acid media, water is discharged (1.23 V/SHE under standard conditions) on the electrode producing adsorbed hydroxyl radicals (1.10), which are the main reaction intermediates for O_2 evolution (1.11).



The reactivity of these electrolytic hydroxyl radicals is very different from the chemically bonded hydroxyl radicals formed by the dissociative activation of water (1.9).

Even if the exact nature of the interactions between the electrolytically generated hydroxyl radicals (1.10) and the electrode surface (M) is not known, we can consider that these hydroxyl radicals are physisorbed on the anode surface.

The EOTR between an organic compound R (supposed none adsorbed on the anode) and the hydroxyl radicals (loosely adsorbed on the anode) takes place close to the anode's surface:



where n is the number of electrons involved in oxidation reaction of R.

1.4 Influence of Anode Material on the Reactivity of Electrolytic Hydroxyl Radicals

The reaction of organics with electrogenerated electrolytic hydroxyl radicals (1.12) is in competition with the side reaction of the anodic discharge of these radicals to oxygen (1.11). The activity [rate of reaction (1.11) and (1.12)] of these electrolytic hydroxyl radicals are strongly linked to their interaction with the electrode surface M. As a general rule, the weaker the interaction, the lower is the electrochemical activity [reaction (1.11) is slow] toward oxygen evolution (high O_2 overvoltage anodes) and the higher is the chemical reactivity toward organics oxidation. Based on this approach, we can classify the different anode materials according to their oxidation power in acid media as it is shown in Table 1.2. This table shows that the oxidation potential of the anode (which corresponds to the onset potential of oxygen evolution) is directly related to the overpotential for oxygen evolution and to the adsorption enthalpy of hydroxyl radicals on the anode surface, i.e., for a given anode material the higher is the O_2 overvoltage the higher is its oxidation power.

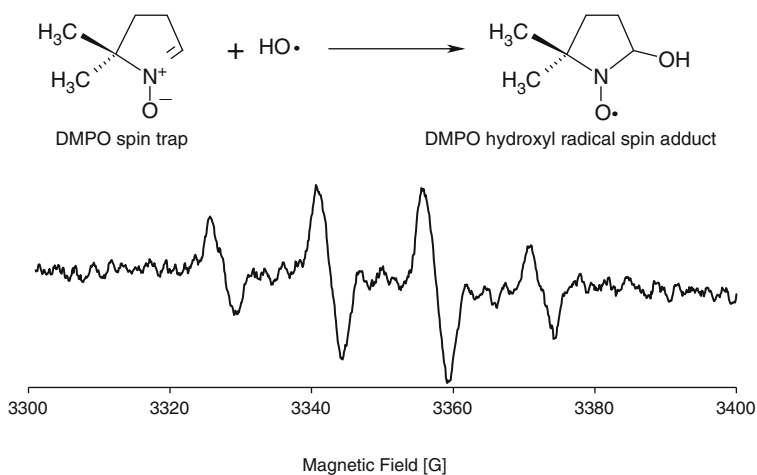
A low oxidation power anode is characterized by a strong electrode–hydroxyl radical interaction resulting in a high electrochemical activity for the oxygen evolution reaction (low overvoltage anode) and to a low chemical reactivity for organics oxidation (low current efficiency for organics oxidation). A typical low oxidation power anode is the IrO_2 -based electrode (Fóti et al. 1999). Concerning this anode, it has been reported that the interaction between IrO_2 and hydroxyl radical is so strong that a higher oxidation state of oxide IrO_3 can be formed. This higher oxide can act as mediator for both organics oxidation and oxygen evolution.

In contrast to this low oxidation power anode, the high oxidation power anode is characterized by a weak electrode–hydroxyl radical interaction resulting in a low electrochemical activity for the oxygen evolution reaction (high overvoltage anode) and to a high chemical reactivity for organics oxidation (high current efficiency for organics oxidation).

Boron-doped diamond-based anode (BDD) is a typical high oxidation power anode (Fóti and Comninellis 2004). By means of spin trapping, the evidence for the formation of hydroxyl radicals on BDD is found (Marselli et al. 2003). The

Table 1.2 Oxidation power of the anode material in acid media

Electrode	Oxidation potential (V)	Overpotential of O ₂ evolution (V)	Adsorption enthalpy of M-OH	Oxidation power of the anode
RuO ₂ -TiO ₂ (DSA-Cl ₂)	1.4–1.7	0.18	Chemisorption of OH radical ↑ ↓ of OH radical	
IrO ₂ -Ta ₂ O ₅ (DSA-O ₂)	1.5–1.8	0.25		
Ti/Pt	1.7–1.9	0.3		
Ti/PbO ₂	1.8–2.0	0.5		
Ti/SnO ₂ -Sb ₂ O ₅	1.9–2.2	0.7		
p-Si/BDD	2.2–2.6	1.3		

**Fig. 1.2** ESR of DMPO adduct obtained after electrolysis of 8.8 mM DMPO solution in 1 M HClO₄ for 2 h on BDD electrode at 0.1 mA cm⁻²

ESR (Electron Spin Resonance) spectrum (Fig. 1.2) recorded during electrolysis of DMPO (5,5 dimethyl-1-pyrroline-N-oxide) solution on BDD confirms the formation of OH during anodic polarization of diamond electrodes. It has been reported that the BDD–hydroxyl radical interaction is so weak (no free p or d orbitals on BDD) that the OH can even be considered as quasi-free. These quasi-free hydroxyl

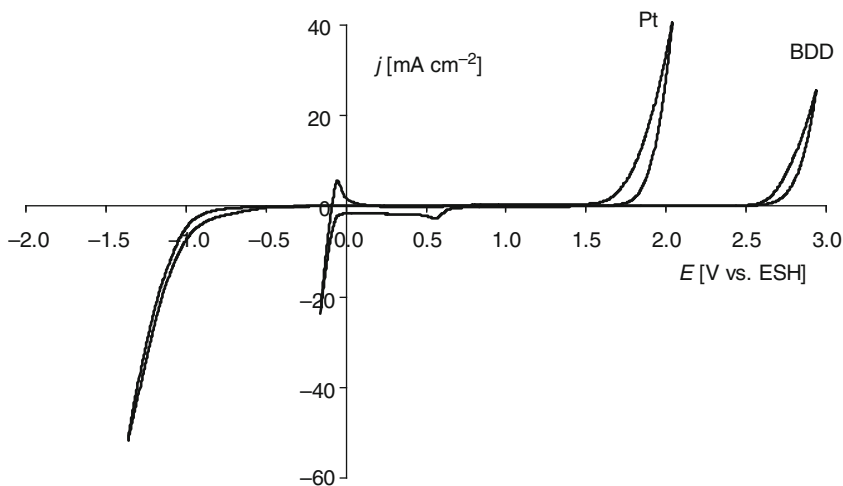
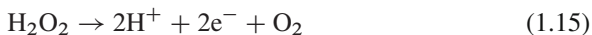


Fig. 1.3 Cyclic voltammograms of BDD and platinum electrodes

radicals are very reactive and can result in the mineralization of the organic compounds (1.13):



Furthermore, BDD anodes have a high overpotential for the oxygen evolution reaction compared with the platinum anode (Fig. 1.3). This high overpotential for oxygen evolution at BDD electrodes is certainly related to the weak BDD–hydroxyl radical interaction, what results in the formation of H_2O_2 near to the electrode's surface (1.14), which is further oxidized at the BDD anode (1.15):



In fact H_2O_2 has been detected during electrolysis in $HClO_4$ using BDD anodes as it is shown in Fig. 1.4 (Michaud et al. 2003).

1.5 Determination of the Current Efficiency of the Electrochemical Mineralization

For the determination of the current efficiency of organics mineralization we consider two parallel reactions:

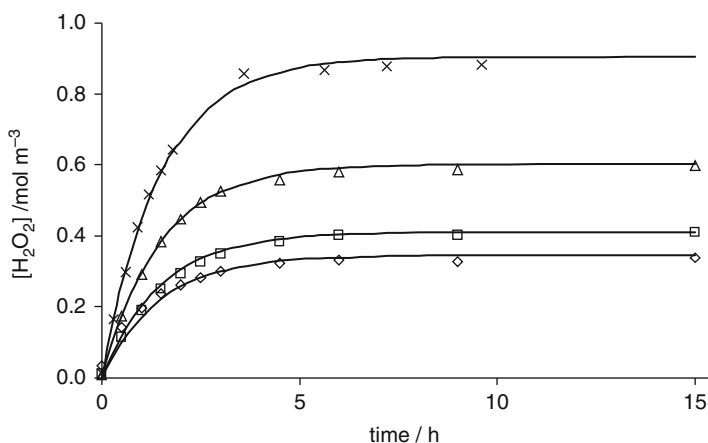
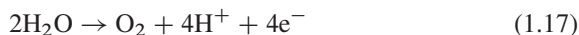


Fig. 1.4 Production of H₂O₂ at different current densities; (open diamond) 230 A cm⁻², (open square) 470 A cm⁻², (open triangle) 950 A cm⁻², (cross) 1,600 A cm⁻² during electrolysis of 1 M HClO₄ on BDD electrode

(a) The main reaction of oxygen transfer from water toward the organic compound



(b) The side reaction of oxygen evolution



In the basis of this simplified reaction scheme, two techniques have been proposed for the estimation of the instantaneous current efficiency (ICE) during electrolysis: the chemical oxygen demand (COD) and the oxygen flow rate (OFR) techniques.

1.5.1 Determination of ICE by the Chemical Oxygen Demand Technique

In this technique, the COD of the electrolyte is measured at regular intervals (Δt) during constant current (galvanostatic) electrolysis and the instantaneous current efficiency (ICE_{COD}) is calculated using the relation:

$$\text{ICE}_{\text{COD}} = \frac{FV}{8I} \frac{[(\text{COD})_t - (\text{COD})_{t+\Delta t}]}{\Delta t}, \quad (1.18)$$

where $(\text{COD})_t$ and $(\text{COD})_{t+\Delta t}$ are the chemical oxygen demand (mol O₂ m⁻³) at time t and $t + \Delta t$ (s), respectively; I is the applied current (A); F is Faraday's constant (C mol⁻¹); and V is the volume of the electrolyte (m³).

1.5.2 Determination of ICE by the Oxygen Flow Rate Technique

In the OFR technique, the OFR is measured continuously in the anodic compartment during constant current (galvanostatic) electrolysis in a two-compartment electrochemical cell. The instantaneous current efficiency (ICE_{OFR}) is then calculated using the relation:

$$ICE_{\text{OFR}} = \frac{\dot{V}_0 - (\dot{V}_t)_{\text{org}}}{\dot{V}_0}, \quad (1.19)$$

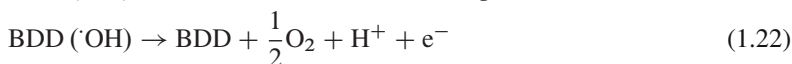
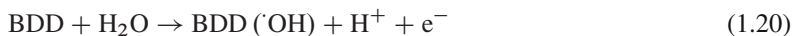
where \dot{V}_0 ($\text{m}^{-3}\text{s}^{-1}$) is the theoretical OFR calculated from Faraday's law (or measured in a blank experiment in the absence of organic compounds) and $(\dot{V}_t)_{\text{org}}$ ($\text{m}^{-3}\text{s}^{-1}$) is the OFR obtained during electrochemical treatment of the wastewater.

Both the COD and OFR techniques have their limitations as given below:

- If volatile organic compounds (VOC) are present in the waste water only the OFR technique will give reliable results.
- If for example Cl_2 (g) is evolved during the treatment (due to the oxidation of Cl^- present in the wastewater) only the COD technique will give reliable results.
- If insoluble organic products are formed during the treatment (for example polymeric material) only the OFR technique will give reliable results.
- Furthermore, simultaneous application of both the COD and OFR techniques during the electrochemical process will allow a better control of the side reactions involved in the electrochemical treatment.

1.6 Kinetic Model of Organics Mineralization on BDD Anode

In this section, a kinetic model of electrochemical mineralization of organics (RH) on BDD anodes under electrolysis regime is presented. In this regime, as reported in Sect. 1.4, electrogenerated hydroxyl radicals (1.20) are the intermediates for both the main reaction of organics oxidation (1.21) and the side reaction of oxygen evolution (1.22).

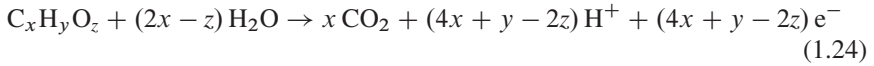


Considering this simplified reaction scheme (1.20)–(1.22), a kinetic model is proposed based on following assumptions: (1) adsorption of the organic compounds at the electrode surface is negligible; (2) all organics have the same diffusion coefficient D ; and (3) the global rate of the electrochemical mineralization of organics is a fast reaction and it is controlled by mass transport of organics to the anode surface.

The consequence of this last assumption is that the rate of the mineralization reaction is independent on the chemical nature of the organic compound present in the electrolyte. Under these conditions, the limiting current density for the electrochemical mineralization of an organic compound (or a mixture of organics) under given hydrodynamic conditions can be written as (1.23)

$$i_{\text{lim}} = nFk_m C_{\text{org}}, \quad (1.23)$$

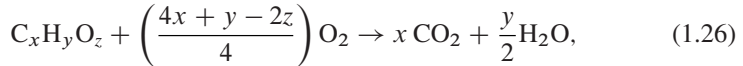
where i_{lim} is the limiting current density for organics mineralization (A m^{-2}), n is the number of electrons involved in organics mineralization reaction, F is Faraday's constant (C mol^{-1}), k_m is the mass transport coefficient (m s^{-1}), and C_{org} is the concentration of organics in solution (mol m^{-3}). For the electrochemical mineralization of a generic organic compound, it is possible to calculate the number of exchanged electrons, from the following electrochemical reaction



Replacing the value of $n = (4x + y - 2z)$ in (1.23) we obtain

$$i_{\text{lim}} = (4x + y - 2z) F k_m C_{\text{org}}. \quad (1.25)$$

From the equation of the chemical mineralization of the organic compound (1.26)



it is possible to obtain the relation between the organics concentration (C_{org} in $\text{mol C}_x\text{H}_y\text{O}_z \text{ m}^{-3}$) and the chemical oxygen demand (COD in $\text{mol O}_2 \text{ m}^{-3}$):

$$C_{\text{org}} = \frac{4}{(4x + y - 2z)} \text{COD}. \quad (1.27)$$

From (1.25) and (1.27) and at given time t during electrolysis, we can relate the limiting current density of the electrochemical mineralization of organics with the COD of the electrolyte (1.28):

$$i_{\text{lim}}(t) = 4Fk_m \text{COD}(t). \quad (1.28)$$

At the beginning of electrolysis, at time $t = 0$, the initial limiting current density (i_{lim}^0) is given by

$$i_{\text{lim}}^0 = 4Fk_m \text{COD}^0, \quad (1.29)$$

where COD^0 is the initial chemical oxygen demand.

Let us define a characteristic parameter α of the electrolysis process (1.30):

$$\alpha = i / i_{\text{lim}}^0. \quad (1.30)$$

Working under galvanostatic conditions α is constant, and it is possible to identify two different operating regimes: at $\alpha < 1$ the electrolysis is controlled by the applied current, while at $\alpha > 1$ it is controlled by the mass transport control.

(a) Electrolysis under current limited control ($\alpha < 1$):

In this operating regime ($i < i_{\text{lim}}$), the current efficiency is 100% and the rate of COD removal ($\text{mol O}_2 \text{ m}^{-2} \text{ s}^{-1}$) is constant and can be written as (1.31)

$$r = \alpha \frac{i_{\text{lim}}^0}{4F}. \quad (1.31)$$

Using relation (1.29), the rate of COD removal (1.31) can be given by

$$r = \alpha k_{\text{m}} \text{COD}^0. \quad (1.32)$$

It is necessary to consider the mass balances over the electrochemical cell and the reservoir to describe the temporal evolution of COD in the batch recirculation reactor system given in Fig. 1.5. Considering that the volume of the electrochemical reactor V_{E} (m^3) is much smaller than the reservoir volume V_{R} (m^3), we can obtain from the mass balance on COD for the electrochemical cell the following relation:

$$Q \text{COD}_{\text{out}} = Q \text{COD}_{\text{in}} - \alpha k_{\text{m}} A \text{COD}^0, \quad (1.33)$$

where Q is the flow rate ($\text{m}^3 \text{ s}^{-1}$) through the electrochemical cell; COD_{in} and COD_{out} are the chemical oxygen demands ($\text{mol O}_2 \text{ m}^{-3}$) at the inlet and at the outlet of the electrochemical cell, respectively; and A is the anode area (m^2). For the well-mixed reservoir (Fig. 1.5), the mass balance on COD can be expressed as

$$Q (\text{COD}_{\text{out}} - \text{COD}_{\text{in}}) = V_{\text{R}} \frac{d(\text{COD}_{\text{in}})}{dt}. \quad (1.34)$$

Combining (1.33)–(1.34) and replacing COD_{in} by the temporal evolution of chemical oxygen demand, COD, we obtain

$$\frac{d(\text{COD})}{dt} = -\alpha \frac{\text{COD}^0 A k_{\text{m}}}{V_{\text{R}}}. \quad (1.35)$$

Integrating this equation subject to the initial condition $\text{COD} = \text{COD}^0$ at $t = 0$ gives the temporal evolution of $\text{COD}(t)$ in this operating regime ($i < i_{\text{lim}}$):

$$\text{COD}(t) = \text{COD}^0 \left(1 - \alpha \frac{A k_{\text{m}}}{V_{\text{R}}} t \right). \quad (1.36)$$

This behavior persists until a critical time (t_{cr}), at which the applied current density is equal to the limiting current density, what corresponds to:

$$\text{COD}_{\text{cr}} = \alpha \text{COD}^0. \quad (1.37)$$

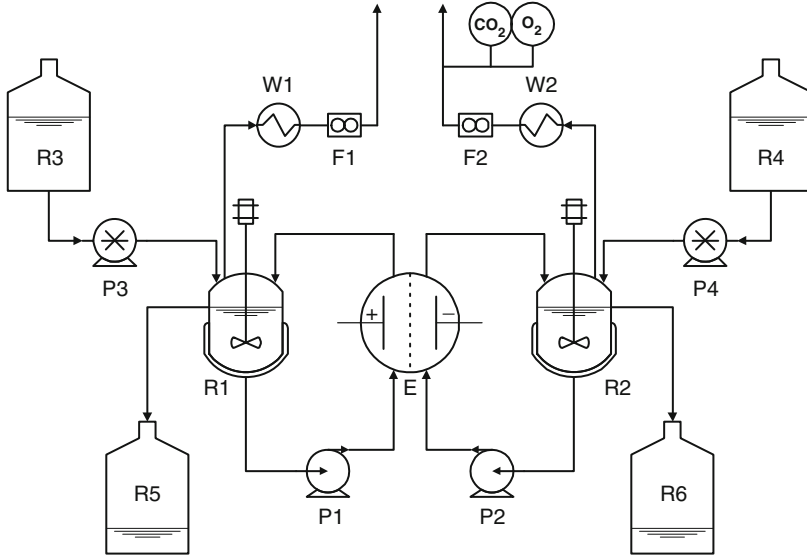


Fig. 1.5 Schematic view of the two-compartment electrochemical flow cell. *R* reservoirs, *P* pumps, *E* electrochemical cell with membrane, *W* heat exchangers, *F* gas flow controllers

Substituting (1.37) in (1.36), it is possible to calculate the critical time:

$$t_{cr} = \frac{1 - \alpha}{\alpha} \frac{V_R}{Ak_m} \quad (1.38)$$

or in term of critical specific charge ($A \cdot h \cdot m^{-3}$):

$$Q_{cr} = i_{lim}^0 \frac{(1 - \alpha)}{k_m \times 3,600} = \frac{4F (\text{COD}^0) (1 - \alpha)}{3,600}. \quad (1.39)$$

(b) Electrolysis under mass transport control ($\alpha > 1$):

When the applied current exceeds the limiting one ($i > i_{lim}$), secondary reactions (such as oxygen evolution) commence resulting in a decrease in the ICE. In this case, the COD mass balances on the anodic compartment of the electrochemical cell *E* and the reservoir *R2* (Fig. 1.5) can be expressed as

$$\frac{d(\text{COD})}{dt} = -\frac{Ak_m \text{COD}}{V_R}. \quad (1.40)$$

Integration of this equation from $t = t_{cr}$ to t , and $\text{COD} = \alpha \text{COD}^0$ to $\text{COD}(t)$ leads to

$$\text{COD}(t) = \alpha \text{COD} \exp\left(-\frac{Ak_m}{V_R} t + \frac{1 - \alpha}{\alpha}\right). \quad (1.41)$$

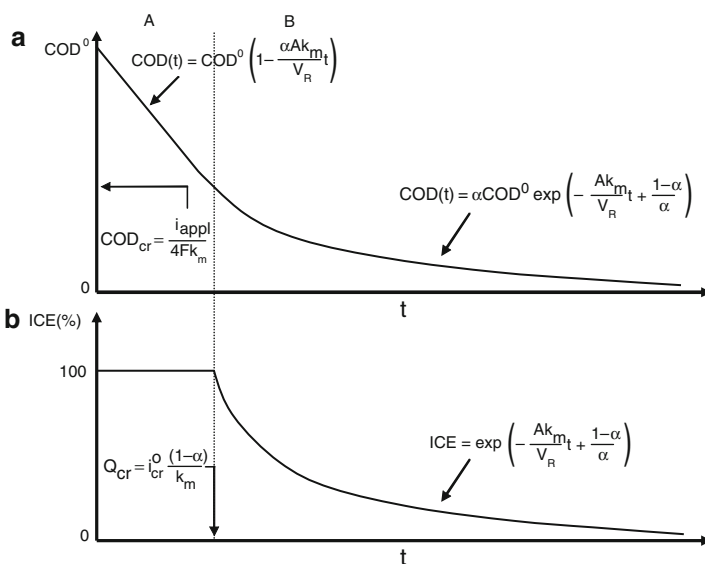


Fig. 1.6 Evolution of (a) COD and (b) ICE in function of time (or specific charge); A represents the charge transport control; B represents the mass transport control

The ICE can be defined as

$$ICE = \frac{i_{lim}}{i} = \frac{COD(t)}{\alpha COD^0}. \quad (1.42)$$

And from (1.41) and (1.42), ICE it is now given by

$$ICE = \exp\left(-\frac{Ak_m}{V_R}t + \frac{1-\alpha}{\alpha}\right). \quad (1.43)$$

A graphical representation of the proposed kinetic model is given in Fig. 1.6. In order to verify the validity of this model, the anodic oxidation of various aromatic compounds in acidic solution has been performed varying organics concentration and current density.

1.6.1 Influence of the Nature of Organic Pollutants

Figure 1.7 shows both the experimental and predicted values (continuous line) of both the ICE and COD evolution with the specific electrical charge passed during the anodic oxidation of different classes of organic compounds (acetic acid, isopropanol, phenol, 4-chlorophenol, 2-naphtol). This figure demonstrates that the

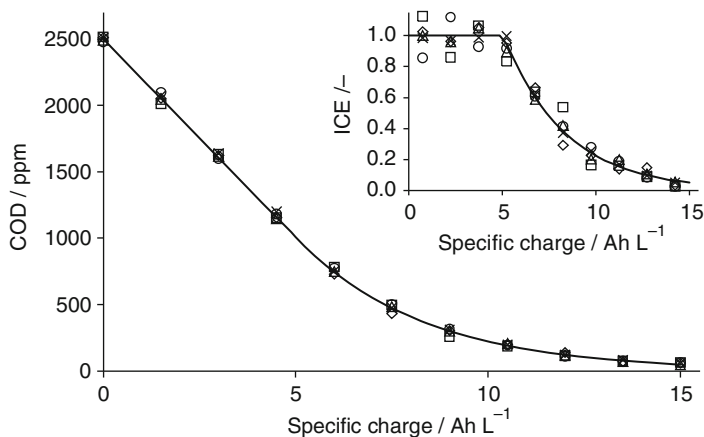


Fig. 1.7 Evolution of COD and ICE (*inset*) in function of specific charge for different organic compounds: (*cross*) acetic acid, (*open square*) isopropanol, (*open circle*) phenol, (*open triangle*) 4-chlorophenol, (*open diamond*) 2-naphtol; $i = 238 \text{ A m}^{-2}$; $T = 25^\circ\text{C}$; Electrolyte: $1 \text{ M H}_2\text{SO}_4$. The *solid line* represents model prediction

electrochemical treatment is independent on the chemical nature of the organic compound. Furthermore, there is an excellent agreement between the experimental data and the predicted values from proposed model.

1.6.2 Influence of Organic Concentration

Figure 1.8 presents both ICE and COD evolution with the specific electrical charge passed during the galvanostatic oxidation (238 A m^{-2}) of 2-naphtol ($2 - 9 \text{ mM}$) in $1 \text{ M H}_2\text{SO}_4$. As predicted from the model, the critical specific charge Q_{cr} (1.39) increases with increase in the initial organic concentration (reported as initial COD^0). Again, there is an excellent agreement between the experimental and predicted values.

1.6.3 Influence of Applied Current Density

The influence of current density on both ICE and COD evolution with the specific electrical charge passed during the galvanostatic oxidation of a 5 mM 2-naphtol in $1 \text{ M H}_2\text{SO}_4$ at different current densities ($119 - 476 \text{ A m}^{-2}$) is shown in Fig. 1.9. As previously noted, an excellent agreement between the experimental and predicted values is observed.

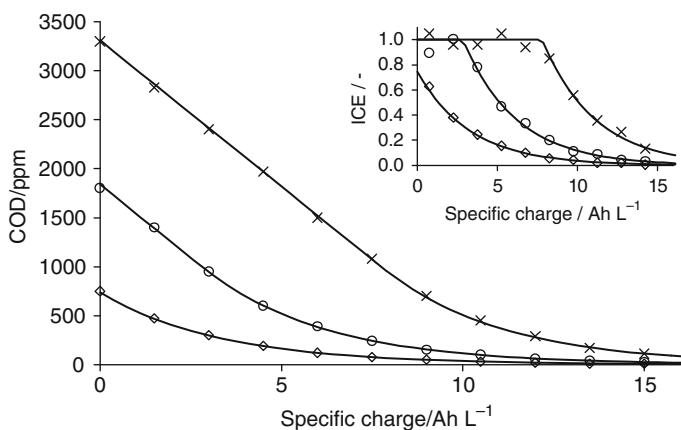


Fig. 1.8 Influence of the initial 2-naphtol concentration: (*cross*) 9 mM, (*open circle*) 5 mM, (*open diamond*) 2 mM on the evolution of COD and ICE (*inset*) during electrolysis on BDD; $i = 238 \text{ A m}^{-2}$; $T = 25^\circ\text{C}$; Electrolyte: 1 M H_2SO_4 . The *solid line* represents model prediction

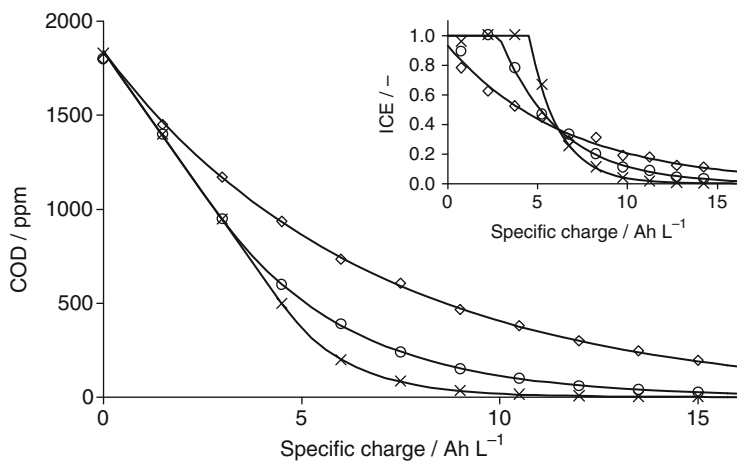


Fig. 1.9 Influence of the applied current density: (*cross*) 119 A m^{-2} , (*open circle*) 238 A m^{-2} , (*open diamond*) 476 A m^{-2} on the evolution of COD and ICE (*inset*) during electrolysis of 5 mM 2-naphtol in 1 M H_2SO_4 on BDD; $T = 25^\circ\text{C}$. The *solid line* represents model prediction

1.7 Intermediates Formed During the Electrochemical Mineralization Process Using BDD

It has been found, that the amount and nature of intermediates formed during the electrochemical mineralization of organics on BDD anodes depends strongly on the working regime. In fact, electrolysis under conditions of current limited control

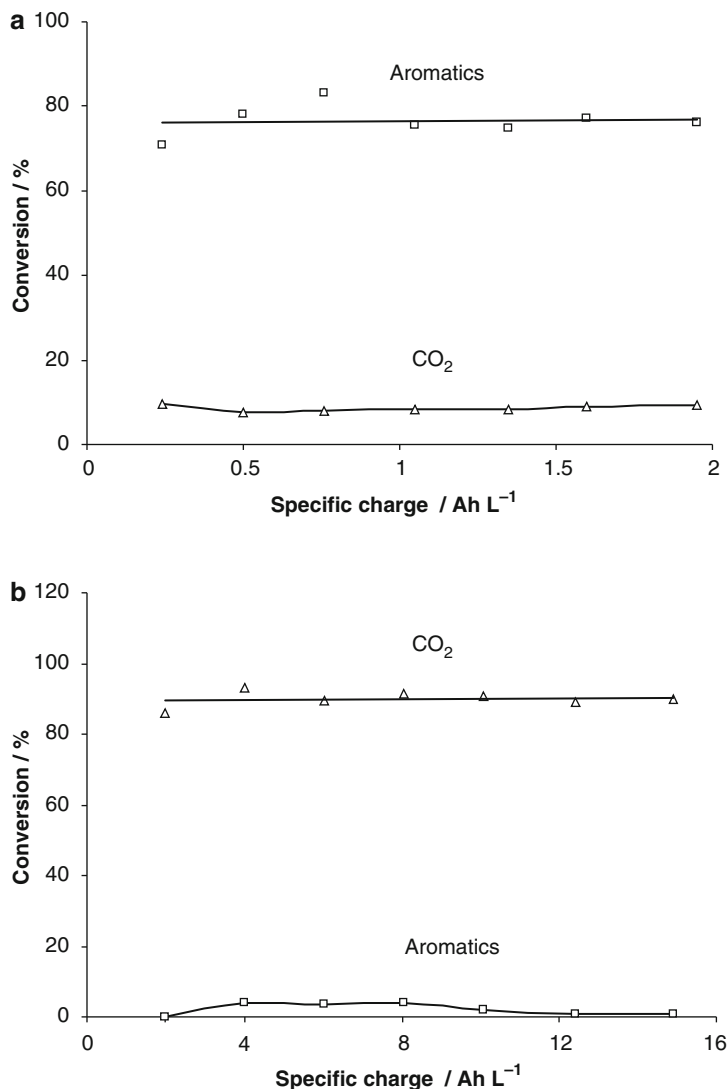


Fig. 1.10 Trend of the percentage of phenol converted to CO₂ (*open triangle*) and to aromatic compounds (*open square*) during phenol electrolysis in 1 M HClO₄ on BDD under (a) current limited control, initial phenol concentration: 20 mM, current density 5 mA cm⁻²; (b) mass transport control, initial phenol concentration: 5 mM, current density 60 mA cm⁻²

results usually in the formation of an important number of intermediates in contrast to electrolysis under mass transport regime, where practically no intermediates are formed and CO₂ is the only final product. Figure 1.10 shows a typical example of phenol oxidation under conditions of current limited control (formation of aromatic intermediates) and mass transport regime (no intermediates, only CO₂).

1.8 Electrical Energy Consumption in the Electrochemical Mineralization Process

In contrast to the chemical oxidation process in which strong oxidants (usually in the presence of catalysts) are used in order to achieve efficient treatment, the electrochemical process consumes mainly electrical energy. The specific energy consumption for the electrochemical treatment of a given wastewater can be estimated from the relation (Panizza et al. 2001a, b):

$$E_{\text{sp}} = \frac{4FV_c}{3,600\text{EOI}} \quad \text{with } 0 \leq \text{EOI} \leq 1, \quad (1.44)$$

where E_{sp} is the specific energy consumption (kWh/kmol COD), F is Faraday's constant (C mol^{-1}), V_c is the cell potential (V), and EOI is the electrochemical oxidation index (which represents the average current efficiency for organics oxidation) given by (1.45):

$$\text{EOI} = \frac{\int_0^\tau \text{ICE} dt}{\tau} \quad \text{with } 0 \leq \text{EOI} \leq 1, \quad (1.45)$$

where ICE is the instantaneous current efficiency (–) and τ is the duration of the electrochemical treatment (s). Using the numerical values, (1.44) can be written as

$$E_{\text{sp}} = 107.2 \frac{V_c}{\text{EOI}} \quad \text{with } 0 \leq \text{EOI} \leq 1. \quad (1.46)$$

The cell potential can be related to the current density by the relation (1.47):

$$V_c = V_0 + \rho di, \quad (1.47)$$

where V_0 is a constant depending on the nature of the electrolyte (V), ρ is the resistivity of the electrolyte ($\Omega \text{ m}$), d is the interelectrode distance (m), and i is the current density (A m^{-2}). Combining (1.46) and (1.47) we obtain

$$E_{\text{sp}} = 107.2 \frac{(V_0 + \rho di)}{\text{EOI}} \quad \text{with } 0 \leq \text{EOI} \leq 1. \quad (1.48)$$

This relation shows that the specific energy consumption decreases with increasing average current efficiency reaching a minimum value at $\text{EOI} = 1$.

1.9 Optimization of the Electrochemical Mineralization Using BDD Anodes

As it has been shown in Sect. 1.8, the specific energy consumption for the electrochemical mineralization of organics decreases strongly with increasing average current efficiency (EOI) and reaches a minimum value at $\text{EOI} = 1$. In order to work

under these favorable conditions (at which $EOI = 1$), electrolysis has to be carried out under programmed current, in which the current density during electrolysis is adjusted to the limiting value. The following steps are proposed for an optimal treatment of a wastewater using BDD anodes:

- (a) Measure the initial chemical oxygen demand (COD^0) of the wastewater.
- (b) Estimate the mass transfer coefficient (k_m) of the electrolytic cell under fixed hydrodynamic conditions (stirring rate). This can be achieved using a given concentration of $Fe(CN)_6^{4-}$ (50 mM) in a supporting electrolyte (1M Na_2SO_4) and measuring the limiting current (I_{lim}) for the anodic oxidation of $Fe(CN)_6^{4-}$ under fixed stirring rate. The mass transfer coefficient (k_m) can then be calculated using the relation:

$$k_m = \frac{I_{lim}}{FA [Fe(CN)_6^{4-}]}, \quad (1.49)$$

where k_m is the mass transfer coefficient ($m s^{-1}$), I_{lim} is the limiting current (A), $[Fe(CN)_6^{4-}]$ is the concentration of $Fe(CN)_6^{4-}$ ($mol m^{-3}$), F is Faraday's constant ($C mol^{-1}$), and A is the anode surface area (m^2).

- (c) Estimate the initial limiting current density (i_{lim}) for the electrochemical mineralization using (1.29).
- (d) Calculate the time constant of the electrolytic cell (τ_c) using the relation:

$$\tau_c = \frac{V_R}{Ak_m}, \quad (1.50)$$

where τ_c is the electrolytic cell time constant (s) and V_R is the volume of the reservoir R2 in Fig. 1.5 (m^3).

- (e) Using (1.29), (1.41), (1.50) and considering $\alpha = 1$ (initial applied current density = calculated initial limiting current density), we obtain the theoretical temporal evolution of the limiting current during electrolysis (1.51).

$$i_{lim} = i_{lim}^0 \exp\left(-\frac{t}{\tau_c}\right). \quad (1.51)$$

- (f) Start electrolysis by application of a current density corresponding to the limiting value [calculated as in point (c)].
- (g) Adjust the current density during electrolysis to the time dependent limiting value according to (1.51).
- (h) From (1.29) and (1.51), calculate the electrolysis time (τ) in order to achieve the target final COD value (COD_{final}) using the relation:

$$\tau = -\tau_c \log \frac{COD_{final}}{COD^0}. \quad (1.52)$$

Table 1.3 Corrosion rate and current efficiency of BDD corrosion for various electrolytes

Electrolyte	Corrosion rate ($\mu\text{g}/\text{Ah}$)	Current efficiency (%)
1M HClO ₄	0.3 \pm 0.1	0.0003
1M H ₂ SO ₄	<0.3	<0.0003
1M H ₂ SO ₄ + 9M CH ₃ OH	3 \pm 1	0.003
1M H ₂ SO ₄ + 3M CH ₃ COOH	12 \pm 2	0.011

1.10 Fouling and Corrosion of BDD Anodes

One of the major problems in the application of the electrochemical technology for wastewater treatment is the fouling of the electrode's surface caused by the deposition of oligomeric or polymeric material and the electrode's deactivation. It has been reported, that BDD electrodes are not sensible to fouling due to the electro-generation of active, electrolytic hydroxyl radicals which can oxidize any polymeric material deposited on the anode's surface. However, BDD anodes are susceptible to deactivation mainly due to the anodic corrosion. The corrosion rate depends strongly on the reaction media as it is shown in Table 1.3. In the same table, the current efficiency of BDD corrosion is also given, considering (1.53).



References

- Bellagamba, R., Michaud, P.-A., Comninellis, Ch. and Vatisstas, N. (2002) Electro-combustion of polyacrylates with boron-doped diamond anodes. *Electrochem. Commun.* 4, 171–176.
- Boye, B., Michaud, P.-A., Marselli, B., Dieng, M.M., Brillas, E. and Comninellis, Ch. (2002) Anodic oxidation of 4-chlorophenoxyacetic acid on synthetic boron-doped diamond electrodes. *New Diam. Front. Carbon Technol.* 12, 63–72.
- Boye, B., Brillas, E., Marselli, B., Michaud, P.-A., Comninellis, Ch. and Dieng, M.M. (2004) Electrochemical decontamination of waters by advanced oxidation processes (AOPS): Case of the mineralization of 2,4,5-T on BDD electrode. *Bull. Chem. Soc. Ethiop.* 18, 205–214.
- Boye, B., Brillas, E., Marselli, B., Michaud, P.-A., Comninellis, Ch., Farnia, G. and Sandonà, G. (2006) Electrochemical incineration of chloromethylphenoxy herbicides in acid medium by anodic oxidation with boron-doped diamond electrodes. *Electrochim. Acta* 51, 2872–2880.
- Brillas, E., Boye, B., Sires, I., Garrido, J.A., Rodriguez, R.M., Arias, C., Cabot, P.-L. and Comninellis, Ch. (2004) Electrochemical destruction of chlorophenoxy herbicides by anodic oxidation and electro-Fenton using a boron-doped diamond electrode. *Electrochim. Acta* 49, 4487–4496.
- Chen, X., Gao, F., Chen, G. and Yue, P.L. (2003) High-performance Ti/BDD electrodes for pollutants oxidation. *Environ. Sci. Technol.* 37, 5021–5026.
- Chen, X., Gao, F. and Chen, G. (2005) Comparison of Ti/BDD and Ti/SnO₂-Sb₂O₅ electrodes for pollutants oxidation. *J. Appl. Electrochem.* 35, 185–191.

- Comninellis, Ch. (1992) Electrochemical treatment of wastewater. *Gas Wasser Abwasser* 72, 792–797.
- Comninellis, Ch. (1994) Electrocatalysis in the electrochemical conversion/combustion of organic pollutants for waste water treatment. *Electrochim. Acta* 39, 1857–1862.
- Comninellis, Ch. and De Battisti, A. (1996) Electrocatalysis in anodic oxidation of organics with simultaneous oxygen evolution. *J. Chim. Phys.* 93, 673–679.
- Comninellis, Ch. and Nerini, A. (1995) Anodic oxidation of phenol in the presence of NaCl for wastewater treatment. *J. Appl. Electrochem.* 25, 23–28.
- Comninellis, Ch. and Plattner, E. (1988) Electrochemical wastewater treatment. *Chimia* 42, 250–252.
- Comninellis, Ch. and Pulgarin, C. (1991) Anodic oxidation of phenol for wastewater treatment. *J. Appl. Electrochem.* 21, 703–708.
- Comninellis, Ch. and Pulgarin, C. (1993) Electrochemical oxidation of phenol for wastewater treatment using tin dioxide anodes. *J. Appl. Electrochem.* 23, 108–112.
- Fóti, G. and Comninellis, Ch. (2004) Electrochemical oxidation of organics on iridium oxide and synthetic diamond based electrodes. In: R.E. White, B.E. Conway, C.G. Vayenas and M.E. Gamboa-Adelco (Eds.), *Modern Aspects of Electrochemistry*, Vol. 37. Plenum, New York, NY, pp. 87–130.
- Fóti, G., Gandini, D. and Comninellis, Ch. (1997) Anodic oxidation of organics on thermally prepared oxide electrodes. In: M. Armand, J.O'M. Bockris, E.J. Cairns, M. Froment, Z. Galus, Y. Ito, R.F. Savinell, Z.W. Tian, S. Trasatti and T.J. VanderNoot (Eds.), *Current Topics in Electrochemistry*, Vol. 5. Research Trends, Trivandrum, pp. 71–91.
- Fóti, G., Gandini, D., Comninellis, Ch., Perret, A. and Haenni, W. (1999) Oxidation of organics by intermediates of water discharge on IrO₂ and synthetic diamond anodes. *Electrochem. Solid-State Lett.* 2, 228–230.
- Fryda, M., Herrmann, D., Schäfer, L., Klages, C.-P., Perret, A., Haenni, W., Comninellis, Ch. and Gandini, D. (1999) Properties of diamond electrodes for wastewater treatment. *New Diam. Front. Carbon Technol.* 9, 229–240.
- Gandini, D., Mahé, E., Michaud, P.-A., Haenni, W., Perret, A. and Comninellis, Ch. (2000) Oxidation of carboxylic acids at boron-doped diamond electrodes for wastewater treatment. *J. Appl. Electrochem.* 30, 1345–1350.
- Haenni, W., Rychen, P., Fryda, M. and Comninellis, Ch. (2004) Industrial applications of diamond electrodes. *Semiconduct. Semimet.* 77, 149–196.
- Iniesta, J., Michaud, P.-A., Panizza, M. and Comninellis, Ch. (2001a) Electrochemical oxidation of 3-methylpyridine at a boron-doped diamond electrode: Application to electroorganic synthesis and wastewater treatment. *Electrochem. Commun.* 3, 346–351.
- Iniesta, J., Michaud, P.-A., Panizza, M., Cerisola, G., Aldaz, A. and Comninellis, Ch. (2001b) Electrochemical oxidation of phenol at boron-doped diamond electrode. *Electrochim. Acta* 46, 3573–3578.
- Marselli, B., Garcia-Gomez, J., Michaud, P.-A., Rodrigo, M.A. and Comninellis, Ch. (2003) Electrogeneration of hydroxyl radicals on boron-doped diamond electrodes. *J. Electrochem. Soc.* 150, D79–D83.
- Martinez-Huitle, C.A., Quiroz, M.A., Comninellis, Ch, Ferro, S. and De Battisti, A. (2004) Electrochemical incineration of chloranilic acid using Ti/IrO₂, Pb/PbO₂ and Si/BDD electrodes. *Electrochim. Acta* 50, 949–956.
- Michaud, P.-A., Panizza, M., Ouattara, L., Diaco, T., Foti, G. and Comninellis, Ch. (2003) Electrochemical oxidation of water on synthetic boron-doped diamond thin film anodes. *J. Appl. Electrochem.* 33, 151–154.
- Montilla, F., Michaud, P.-A., Morallon, E., Vazquez, J.L. and Comninellis, Ch. (2001) Electrochemical oxidation of benzoic acid on boron doped diamond electrodes. *Portug. Electrochim. Acta* 19, 221–226.
- Montilla, F., Michaud, P.-A., Morallon, E., Vazquez, J.L. and Comninellis, Ch. (2002) Electrochemical oxidation of benzoic acid at boron-doped diamond electrodes. *Electrochim. Acta* 47, 3509–3513.

- Ouattara, L., Duo, I., Diaco, T., Ivandini, A., Honda, K., Rao, T., Fujishima, A. and Comninellis, Ch. (2003) Electrochemical oxidation of ethylenediaminetetraacetic acid (EDTA) on BDD electrodes: Application to wastewater treatment. *New Diam. Front. Carbon Technol.* 13, 97–108.
- Ouattara, L., Chowdhry, M.M. and Comninellis, Ch. (2004) Electrochemical treatment of industrial wastewater. *New Diam. Front. Carbon Technol.* 14, 239–247.
- Panizza, M., Michaud, P.-A., Cerisola, G. and Comninellis, Ch. (2001a) Anodic oxidation of 2-naphthol at boron-doped diamond electrodes. *J. Electroanal. Chem.* 507, 206–214.
- Panizza, M., Michaud, P.-A., Cerisola, G. and Comninellis, Ch. (2001b) Electrochemical treatment of wastewaters containing organic pollutants on boron-doped diamond electrodes: Prediction of specific energy consumption and required electrode area. *Electrochem. Commun.* 3, 336–339.
- Polcaro, A.M., Mascia, M., Palmas, S. and Vacca, A. (2004) Electrochemical degradation of diuron and dichloroaniline at BDD electrode. *Electrochim. Acta* 49, 649–656.
- Polcaro, A.M., Vacca, A., Mascia, M. and Palmas, S. (2005) Oxidation at boron doped diamond electrodes: Effective method to mineralise triazines. *Electrochim. Acta* 50, 1841–1847.
- Pulgarin, C., Adler, N., Peringer, P. and Comninellis, Ch. (1994) Electrochemical detoxification of a 1,4-benzoquinone solution in wastewater treatment. *Water Res.* 28, 887–893.
- Rodrigo, M.A., Michaud P.-A., Duo, I., Panizza, M., Cerisola, G. and Comninellis, Ch. (2001) Oxidation of 4-chlorophenol at boron-doped diamond electrode for wastewater treatment. *J. Electrochem. Soc.* 148, D60–D64.
- Seigneur, C., Pulgarin, C., Peringer, P., Comninellis, Ch. and Plattner, E. (1992) Degradation of industrial organic pollutants. *Electrochemical and biological treatment and combined treatment.* *Swiss Chem.* 14, 25–30.
- Simond, O., Schaller, V. and Comninellis, Ch. (1997) Theoretical model for the anodic oxidation of organics on metal oxide electrodes. *Electrochim. Acta* 42, 2009–2012.
- Zanta, C.L.P.S., Michaud, P.-A., Comninellis, Ch., De Andrade, A.R. and Boodts, J.F.C. (2003) Electrochemical oxidation of p-chlorophenol on SnO₂-Sb₂O₅ based anodes for wastewater treatment. *J. Appl. Electrochem.* 33, 1211–1215.